Wind Tunnel Pressure Measurement Study on A Tall Tapered Rectangular Building under Open Terrain Condition

S.P. Adithya[1] and P. Vasanthi[3]
[1]-M.E. Student (Structural Engg.) and [3]-Assistant Professor
Department of Civil Engineering
Sathyabama University,
Chennai, India

G. Ramesh Babu[2] and P.Harikrishna[4]
[2]-Principal Scientist and [4]-Senior Principal Scientist
Wind Engineering Lab
CSIR-Structural Engineering Research Centre
Chennai, India

***Abstract*—Tall buildings are subjected to high wind-induced responses, predominantly across-wind response. Tapering the cross section can effectively reduce across wind response. Since the design code for wind load IS: 875 (Part 3) provide little guidance for the estimation of wind effects on tapered structures, wind tunnel tests are needed to assess the wind loads on such structures. This paper presents the pressure measurement study on a tall tapered rectangular building model (aspect ratio in plan of 1:2) with base and top dimensions of 10 cm × 20 cm and 5 cm × 10 cm respectively and height 70 cm representing a model scale of 1:300 of 210m tall building. Tests have been conducted under open terrain condition in a boundary layer wind tunnel. The pressure taps have been installed along the circumference of the model at 8 different levels, along the height of the model. Pressure measurements have been made for 13 different angles of wind incidence from 0° to 90°. The evaluated mean drag force coefficients are compared with IS code values for two regular rectangular building for wind directions normal to both smaller and larger face of the building. Further, this paper describes the variation of Mean and Standard Deviation of pressure and force coefficient for various angles of wind incidence at different levels.**

Keywords*—Wind tunnel; open terrain; tapered rectangular building; pressure coefficient; force coefficient.

I. INTRODUCTION

The emerging trends of tall buildings and slender light weight structures made, wind load consideration a prerequisite in the design of tall buildings. Along and across-wind responses becomes higher as the building height increases and sometimes the across-wind response become the predominant design criteria. The across-wind response can be reduced by aerodynamic modification of tall buildings by changing the cross section of the building along height such as tapering or setback.

Generally, wind load acting on a building is obtained by using the pressure or force coefficient given in Indian Standard code IS: 875 (part-3) – 1987 on Wind loads. These coefficients are the results of the building obtained in smooth flow conditions. In reality, structures exist in the atmospheric boundary layer subjected to turbulent shear flow conditions. Also, wind can act at any angle to the building axis and this directionality factor is not considered in the present code.

In the past, many wind tunnel studies available in literature have been done on tapered square sections. Young-Moon Kima, Ki-PyoYoua and Nag-Ho Kob (2008) investigated the effect of tapering on reducing the RMS across wind displacement responses of a tapered tall building. Yongchul Kim and Jun Kanda, (2010) made a study on changes of sectional shapes of tall building through tapered and set back to modify the flow pattern around the model and it resulted in reducing the wind induced excitation. Jiming Xie (2014) assessed the effectiveness of tapering, twisting and stepping. He concluded that by aerodynamically changing the shapes of the building would lead to reduction of across wind response.

In this paper, wind tunnel experimental results on a tall tapered rectangular building (plan ratio 1:2) are discussed in detail. Experiments were conducted in the boundary layer wind tunnel facility at CSIR – SERC. Pressure and force coefficients have been evaluated and their distributions along the circumference and their variations along the height have been studied.

In the tapered tall structure, the shape of the building can be aerodynamically modified by changing the taper of the cross section. This modification alters the flow pattern around the building and reduces wind induced vibration of tall buildings. A tapered tall building that spreads the vortex shedding over a broad range of frequencies, are more effectively reduce across wind responses. For the tapered building, the tapering ratio is defined in (1) as

$$\text{Tapering Ratio (R)} = \frac{\text{Base width} - \text{Top width}}{\text{Building height}} \qquad (1)$$

In the present work, the tapering ratio of the tapered rectangular building has been chosen in such a way that the side ratio is maintained as 1:2 at all levels. The tapering ratio of 14.28% and 7.14% is considered for the longer and shorter face respectively.

II. EXPERIMENTAL STUDIES

A. *Model Fabrication and Instrumentation*

A rigid tall tapered rectangular building model with base and top dimensions of 10cm × 20cm and 5cm × 10cm respectively and height 70cm corresponding to a 1:300 model scale of a 210m high tall building has been used in the present investigation.

The model has been fabricated with 5mm thick acrylic sheets. Pressure taps are drilled around the model at 8 different levels depending upon the various z/H ratios (0.1, 0.2, 0.3, 0.5, 0.7, 0.8, 0.9, 0.95) adopted where H is the total height of the building model including base plate. On face A and C, 5 pressure taps are drilled at each level and for faces B and D, 9 pressure taps are drilled at each level. This gives 28 pressure taps at each level and a total of 224 pressure taps for the entire model. Eight pressure scanners are connected to pressure taps via pressure tubes to form the pressure measurement system. Fig. 1 shows the distribution of pressure ports over the surface of the entire building model. The pressure port location at a typical level on the building model is given in Fig.2.

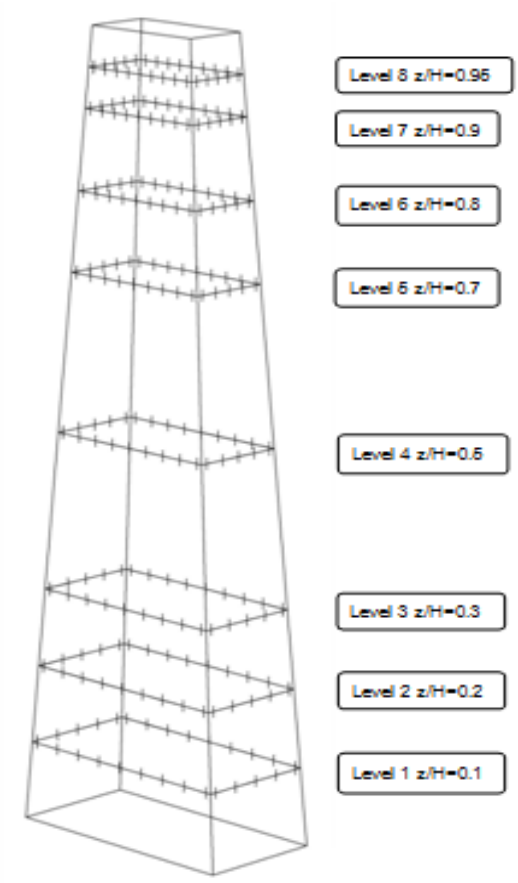

Fig. 1. Schematic representation of pressure ports on building model

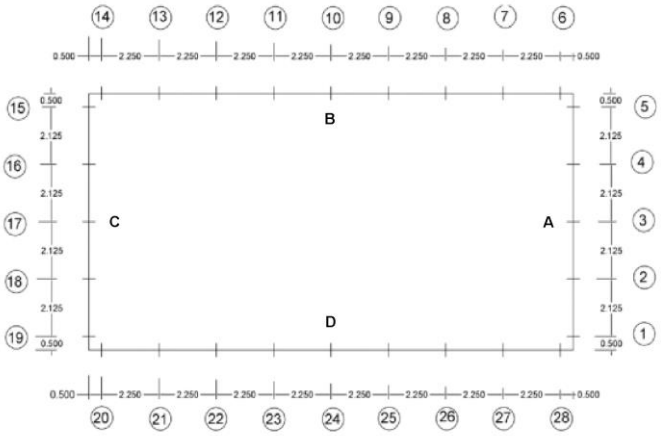

All Dimensions are in cm

Fig. 2. Location of pressure ports at level 1

B. *Wind tunnel experiment*

The completed model is mounted on the wind tunnel turn table at the downstream end of the test section. The building is initially set with its narrow face perpendicular to wind flow direction which represents 0° angle of wind attack as shown in Fig. 3. The model was tested at a wind speed of 14.17m/s corresponding to the model height in the simulated open terrain conditions for 13 different angles of wind incidence namely 0°, 5°, 10°, 15°, 26.5°, 30°, 45°, 60°, 63.5°, 70°, 75°, 80°, and 90°. Three trails were carried out for each angle of wind incidence and the data is acquired at a sampling frequency of 700Hz for a sampling duration of 15s. As mentioned earlier, experiments were conducted in the simulated open terrain condition. The power law exponent for the mean velocity profile was obtained as 0.165. The turbulence intensity at the model height was obtained as 11.5%.

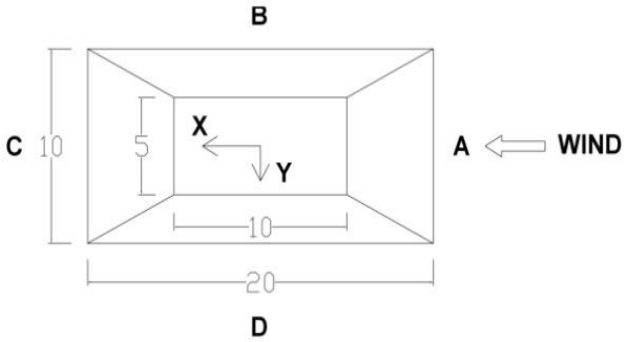

All Dimensions are in cm

Fig. 3. Plan view showing different faces of the model with θ = 0°.

The Fig. 4 and 5 show typical views of instrumented model inside the wind tunnel at CSIR-SERC for 0° and 90° respectively.

Fig. 4. Typical view of the model oriented at θ = 0° in wind tunnel

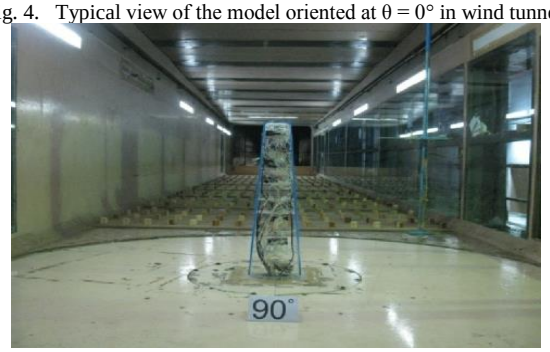

Fig. 5. Typical view of the model oriented at θ = 90° in wind tunnel

III. RESULTS AND DISCUSSIONS

The pressure measurement data of wind tunnel test have been processed for the pressure coefficients and force coefficients using a custom tailored in house program developed in MATLAB software.

The pressure coefficients (Cp) are obtained by processing the pressure data as given below:

$$Cp = \frac{p - p_{static}}{p_{total} - p_{static}} \quad (2)$$

$$p_{total} - p_{static} = p_{ref} = \frac{1}{2}\rho\bar{U}_z^2 \quad (3)$$

Where,

p : Measured pressure on the building model surface

p_{static} : Static pressure from pitot

p_{total} : Total pressure from pitot

p_{ref} : Reference dynamic pressure

ρ : Density of air

$\bar{U}_z$: Mean wind velocity at height 'z' of the model.

The integral of pressure over the surface area on which it acts give the wind induced forces on the building at that portion. The forces obtained in both X and Y direction are resolved in the direction of wind and perpendicular to the direction of wind to evaluate the drag force F_D and lift force F_L. These forces are further processed to obtain drag and lift force coefficient as shown in (4) and (5) and the reference width B' and D' rotated through angle θ is given in Fig. 6.

$$\bar{C}_D = \frac{\bar{F}_D}{B'\bar{p}_{ref}} \quad (4)$$

$$\bar{C}_L = \frac{\bar{F}_L}{D'\bar{p}_{ref}} \quad (5)$$

Where,

$\bar{C}_D, \bar{C}_L$ Mean drag and lift force coefficients

$\bar{F}_D, \bar{F}_L$ Mean drag and lift force

B' Reference width at respective level for C_D

D' Reference width at respective level for C_L

$\bar{p}_{ref}$ Reference pressure

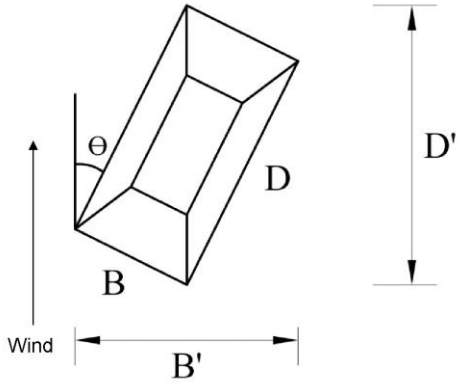

Fig. 6. Projected width when building rotated through an angle θ with respect to wind direction

A. *Normalized Chord length*

In this tapered rectangular building model, the width at each level is varying along height and hence normalized chord length defined in (6) has been used and is given in

Table I.

$$\text{Normalized chord Length} = \frac{\text{Chord length corresponding to each port at a particular level}}{\text{Total chord length (perimeter) at that particular level}} \quad (6)$$

TABLE I. NORMALIZED CHORD LENGTH FOR EACH FACE OF THE BUILDING MODEL

Face	Normalized Chord Length
A	0 – 0.167
B	0.167 – 0.5
C	0.5 – 0.667
D	0.667 – 1

B. *Variation of Mean Pressure Coefficient*

For θ = 0°, it is observed that the values of mean pressure coefficients values are higher for level-1 in comparison with the other levels in face-A as shown in Fig. 7. Since face-B and face-D are two side walls and are symmetric with respect to flow direction, a symmetric distribution can be observed on face-B and face-D. A lower value of mean pressure coefficient of about -0.41 is observed in the wake region (face-C). For θ= 63.5° angle of wind incidence, high positive pressure value of 1.29 was observed at normalized chord length of 0.25 at level-1 as shown in Fig. 8 and in the wake, the mean pressure coefficient varies from -1.0 to -0.6 from

level 1 to 8. For θ = 90° angle of wind incidence, a clear symmetry can be observed in the mean pressure coefficient distribution as shown in Fig.9 and the values of mean pressure coefficient vary from -1.4 to -0.7from level 1 to 8.

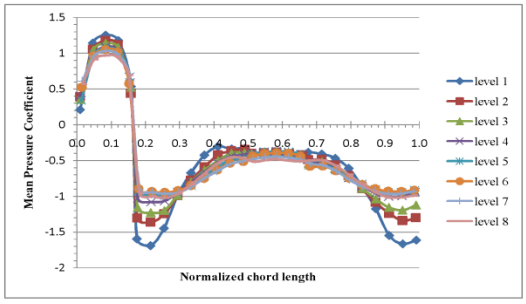

Fig. 7. Variation of mean pressure coefficient with normalized chord length for θ = 0°

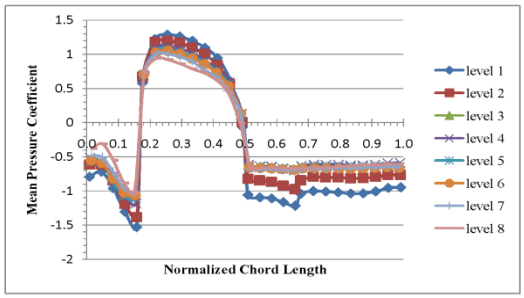

Fig. 8. Variation of mean pressure coefficient with normalized chord length for θ = 63.5°

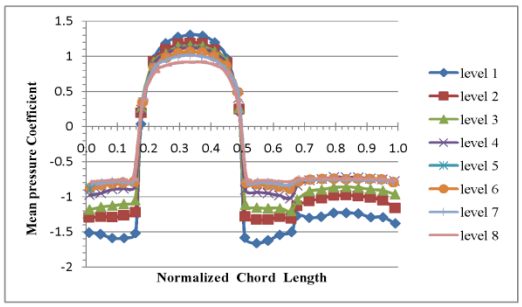

Fig. 9. Variation of mean pressure coefficient with normalized chord length for θ = 90°

C. *Variation of Standard Deviation of Pressure Coefficient*

For θ = 0°, The values of standard deviation of pressure coefficient are increasing with the decrease in height above the tunnel floor, which can be linked to turbulence intensity variation in the approach flow. More recirculation process around the side walls can be observed with more standard deviation values in that region. A standard deviation value of 0.9 is observed in the side face of the model at level 1 as shown in Fig. 10. For θ = 63.5°, The values of standard deviation of pressure coefficient vary from 0.9 to 0.26 between face A and face B as shown in Fig. 11. And for face C, a peak value of 0.54 is observed at a normalized chord length of 0.65. For θ = 90°, a perfect symmetry is observed at a normalized chord length of 0.33. A peak standard deviation value of 0.78 is observed in the side faces A and C as shown in Fig. 12.

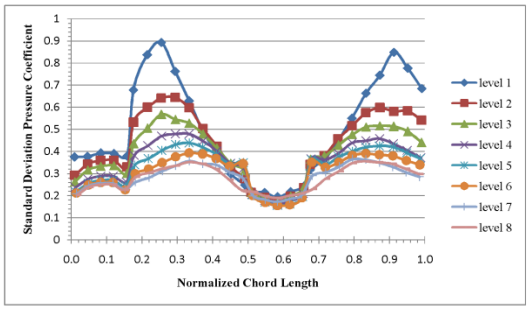

Fig. 10. Variation of standard deviation of pressure coefficient with normalized chord length for θ = 0°

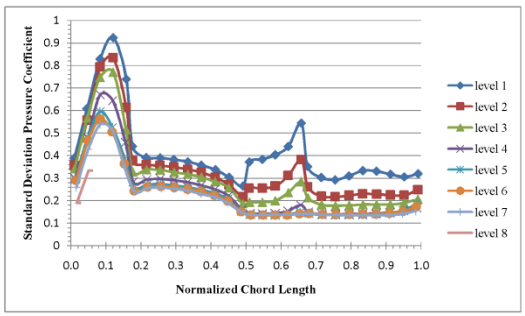

Fig. 11. Variation of standard deviation of pressure coefficient with normalized chord length for θ = 63.5°

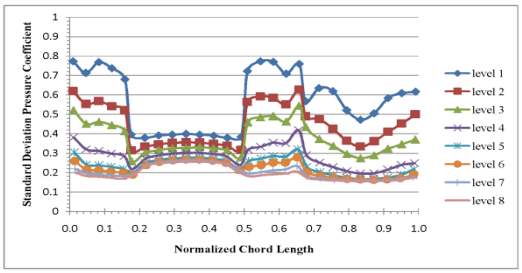

Fig. 12. Variation of standard deviation of pressure coefficient with normalized chord length for θ = 90°

D. *Variation of Mean Drag Force Coefficient*

From Fig. 13, it is observed that the mean drag coefficient obtained at level-1 is always higher than those values at other levels. The mean drag coefficient values varying between 1.23 and 1.35 for 0° angle of wind incidence and between 1.5 and 2.3 for 90° angle of wind incidence. The curve at each level contains three distinct features (i) decreasing trend between θ = 0° to θ = 10° (ii) more or less constant value of mean drag coefficient values between θ = 15° to θ = 60° (iii) increasing trend between θ = 60° to θ = 90°, which can be attributed to distinct flow pattern and their corresponding pressure distribution around the body.

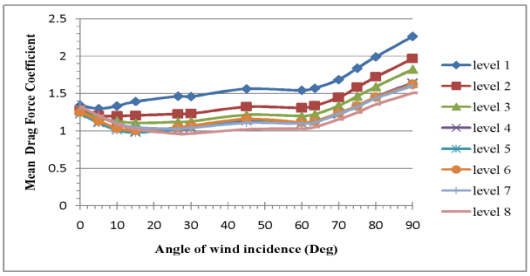

Fig. 13. Variation of mean drag force coefficient with various angles of wind incidence (W_{ref}=B')

E. *Variation of Mean Lift Force Coefficient*

From Fig. 14, it can be observed that the values of mean lift force coefficients are zero at θ = 0° and θ = 90° angles of wind incidences due to symmetry of the cross-section with respect to wind direction. The values of mean lift coefficient are increasing as the angle of wind incidence varying from θ = 0° to θ = 63.5° and a maximum value of 0.64 to 0.95 is observed at an angle of θ = 63.5° for all levels. Further, the mean lift coefficient values are decreasing with angle of wind incidence vary from θ = 63.5° to θ = 90°.

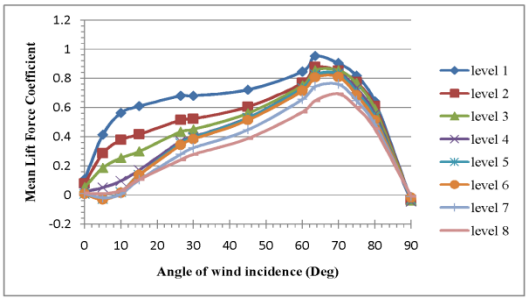

Fig. 14. Variation of mean lift force coefficient with various angles of wind incidence (W_{ref}=D')

F. *Variation of Standard Deviation of Drag Force Coefficient*

The values of standard deviation drag force coefficient are increasing with the change in angle of wind incidence from θ = 0° to θ = 90°. With the change in angle of wind incidence, the projected widths are changing and the aspect ratios are varying, which is having influence on flow characteristics and hence on drag force coefficient values. The values of standard deviation of drag force coefficient are varying between 0.4 and 0.59 for level-1, and in the range of 0.34 to 0.3 in the cases of level- 8 as shown in Fig. 15.

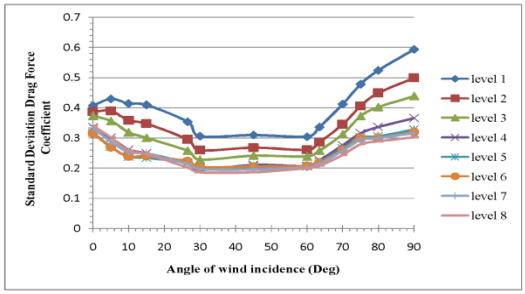

Fig. 15. Variation of standard deviation of drag force coefficient with various angles of wind incidence (W_{ref}=B')

G. *Variation of Standard Deviation of Lift Force Coefficient*

The variation in the values of lift force coefficient is mainly due to the cross-wind turbulence and due to the vortex shedding phenomenon. From this Fig. 16, it is observed that standard deviation for lift force coefficient is found to depend on the turbulence intensity. As height from ground increases, the standard deviation value is reduced. The localized peak in fluctuating lift force coefficient is observed at θ = 63.5°. Higher value is observed at θ = 0° and θ = 90° where the value of mean lift force coefficient is zero. The standard deviation values are varying from 0.27 to 0.53 at θ = 0°, 0.14 to 0.34 at θ = 45°, 0.24 to 0.48 at θ = 63.5° and 0.19 to 1.06 at θ = 90° angles of wind incidences as moving from level-8 to level-1.

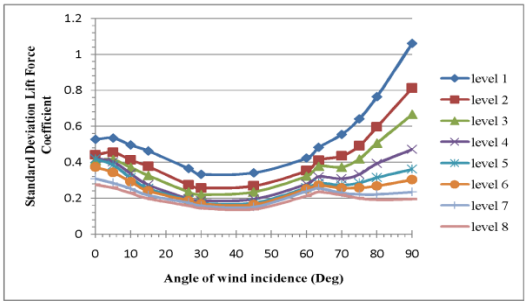

Fig. 16. Variation of standard deviation of lift force coefficient with various angles of wind incidence (W_{ref}=D')

H. *Comparison of Mean Drag Coefficient with Codal Values*

The mean drag coefficients obtained in the present study for the tall tapered rectangular building are compared with the mean drag force coefficients given in the Indian standard code (IS:875(part-3)-1987) for two regular rectangular building RA and RB with uniform cross section along the height. The cross sectional dimensions for RA and RB are equal to the base and top dimensions of the tall tapered rectangular Building respectively and is given in table II.

TABLE II. CROSS SECTIONAL DIMENSIONS FOR RA AND RB

Regular Rectangular Building	Tapered Rectangular Building model	Model Dimension (cm)
RA	Base Dimension	10 × 20
RB	Top Dimension	5 × 10

From the Indian standard code, a uniform drag coefficient value along the height is adopted for both RA and RB. The value of mean drag force coefficients obtained as per Fig. 4 of the IS 875 (Part 3) code for RA and RB are 1.25 and 1.35 for θ= 0° and 1.35 and 1.65 for θ = 90° cases respectively. For θ=0°, the average values of mean drag coefficient obtained from level 4 to 6 is 1.24 for tapered rectangular building model which are in good agreement with RA as shown in Fig. 19. For θ = 90°, the average values of mean drag coefficient obtained from level 4 to 6 is 1.63 for tapered rectangular building model which are in good agreement with RB as shown in Fig. 20.

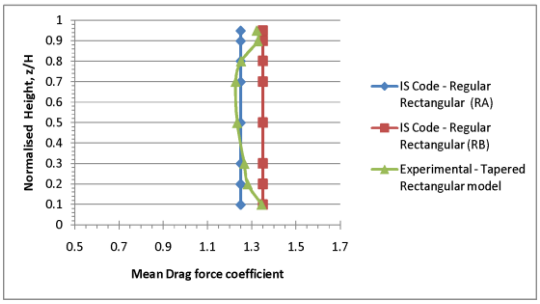

Fig. 17. Comparison of variation of mean drag coefficients with normalized height for θ = 0° angle of wind incidence

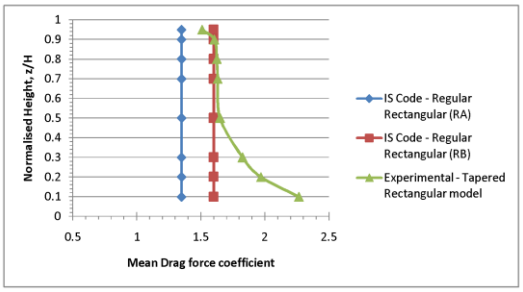

Fig. 18. Comparison of variation of mean drag coefficients with normalized height forθ = 90° angle of wind incidence

IV. CONCLUSION

Distribution of mean pressure coefficients depend upon the flow pattern around the building. Mixing of flow takes place in the wake region which makes the pressure coefficients at all levels to collapse to the same value in the wake. Mean drag and lift force coefficients are found to depend upon the gust buffeting characteristics. Mean force coefficient values for level-1 is always higher than the other levels, due to standing vortex effect at base. The mean force coefficients for level-2 to 8 are observed to be gradually varied along height, which indicates that the force coefficients are primarily controlled by the gust buffeting characteristics. The mean drag coefficient values, obtained in the present study for the open terrain are in good agreement with the Indian code values for building RA for θ = 0° and with RB for θ = 90°. This is because it depends upon the aspect ratio of the building facing the wind.

V. ACKNOWEDGMENT

This paper is being published with kind permission of Director, CSIR- SERC. The help and cooperation rendered by the staff of wind engineering lab in carrying out the experiments are gratefully acknowledged.

VI. REFERENCES

[1] IS: 875 (Part-III)-1987, “Code of Practice for Design Loads” (other than Earthquake) for Buildings and Standards, BIS, New Delhi.
[2] Young-Moon Kima, Ki-Pyo Youa and Nag-Ho Kob (2008) “Across-wind responses of an aeroelastic tapered tall building”. Journal of Wind Engineering and Industrial Aerodynamics. Vol. 96, Pg. no. 1307-1319.
[3] Yongchul Kim and Jun Kanda (2010) “Effects of taper and set-back on wind force and wind-induced response of tall buildings”. Wind and Structures. Vol. 13, No 6, Pg. no. 499-517.
[4] Jiming Xie (2014) “Aerodynamic optimization of super-tall buildings and its effectiveness assessment”. Journal of Wind Engineering and Industrial Aerodynamics. Vol. 130, Pg. no. 88-98.